Heliyon 9 (2023) e19577

Contents lists available at ScienceDirect

Heliyon

journal homepage: www.cell.com/heliyon

Optimization of fluidized bed agglomeration process for developing a blackberry powder mixture

Misael Cortés Rodríguez [a,**], Jesús Humberto Gil G [a], Rodrigo Ortega-Toro [b,*]

[a] Universidad Nacional de Colombia sede Medellín, Facultad Ciencias Agrarias, Departamento Ingeniería Agrícola y Alimentos, Cra. 65 No. 59A – 110, Medellín, CP 050034, Antioquia, Colombia

[b] Universidad de Cartagena, Programa de Ingeniería de Alimentos, Food Packaging and Shelf Life Research Group (FP&SL), Avenida del Consulado Calle 30 No. 48 – 152, Cartagena de Indias D.T. y C., Colombia

ARTICLE INFO

Keywords:
Rubus glaucus benth
Instantization properties
Powder flow
Active components

ABSTRACT

The research objective was to experimentally optimize the fluidized bed agglomeration process of an agglomerated blackberry powder mixture (ABPM) using the response surface methodology. As a raw material, a powdered mixture of blackberry from Castile (*Rubus glaucus* Benth) obtained by spray drying (SD) was used. In the evaluation of the agglomeration process, the response surface methodology was applied using a central design with a face-centered composition ($\alpha = 1$), considering the independent variables: fluidisation air inlet temperature (T) (50–70 °C), the binder solution atomization air pressure (P) (1–2 bar) and process time (t) (20–35 min); and the dependent variable: moisture content (Xw), solubility (S), wettability (*We*), apparent density (ρ_a), total phenols (TP), radical scavenging (ABTS·+ and DPPH· methods), anthocyanins (Ant) (cyanidin-3-glucoside (C_3G)), ellagic acid (EA) and vitamin C (Vit. C). In general, the ABPM exhibited higher porosity and particle size, which generated changes in S, *We* and ρa, and a better rehydration capacity of the ABPM. The optimal process conditions (T = 70 °C, P = 1.7 bar and t = 21.7 min) defined the most favourable attributes of the ABPM (Xw = 9.7 ± 0.1%, S = 74.9 ± 4.9%, *We* = 13.7 ± 3.6 min, $\rho_a = 0.312 \pm 0.009$ g/mL, TP = 4084.6 ± 30.6 mg AGE/100g dry base (db), ABTS·+ = 4511.4 ± 124.5 mg TE/100 g db, DPPH· = 4182.7 ± 66.4 mg TE/100 g db, Ant = 213.6 ± 15.9 mg C_3G/100 g db, EA = 1878.2 ± 45.9 mg/100 g db and Vit. C = 29.8 ± 7.4 mg/100 g db. The agglomeration process improved the instantaneous properties and the flow behaviour of the ABPM. Additionally, it offers significant nutritional value with potential use as an instant drink and raw material for the food industry.

1. Introduction

The blackberry (*Rubus glaucus* Benth) is a fruit from the Rosaceae family in the genus Rubus, commonly referred to as Castile blackberry or Andean blackberry. The blackberry is classified as a type of berry, which is a small round fruit with a sweet flavour [1]. Berries contain the main reservoirs of phenolic compounds, exhibiting antioxidant levels four times higher than those found in other fruits, ten times higher than vegetables, and 40 times higher than cereals [2]. The blackberry is considered a functional food since it has actual contents of vitamins (A, B, C and E), minerals (Ca, Fe, Mg, P, k, Zn, Cu, Se, Na, among others), ellagitannins and

* Corresponding author.
** Corresponding author.
E-mail addresses: mcortesro@unal.edu.co (M. Cortés Rodríguez), rortegap1@unicartagena.edu.co (R. Ortega-Toro).

https://doi.org/10.1016/j.heliyon.2023.e19577
Received 27 May 2022; Received in revised form 23 August 2023; Accepted 27 August 2023
Available online 30 August 2023

proanthocyanidins, hydroxycinnamic acids, flavonoids, and anthocyanins (Ant) (mainly cyanidin-3-*O*-glucoside (C_3G) and cyanidin-3-*O*-rutinoside) [3,4]. This compositional value gives it antioxidant, anti-inflammatory, chemo preventive and antimicrobial properties, in addition to effects on blood lipids and atherosclerosis, being beneficial in preventing chronic diseases such as cancer, cardiovascular diseases, and neurodegenerative disorders [3,5].

The fluidized bed agglomeration (FBA) method allows the assembly of native particles through short-range forces between them, caused by a binding solution (BS) that wets their surfaces, initially forming liquid bridges between the particles, which grow and consolidate until they stabilize the agglomerate during the processing time (t) and inlet air temperature (T). Finally, the agglomerate acquires a higher mechanical resistance through solid bridges and larger size and porosity [6,7]. The FBA process is complex, where various independent variables (IV): charge size, mass charge/mass BS ratio, t, T, pressure or airflow, the concentration of fluidizers, BS flow, air pressure at the inlet nozzle of the BS, the concentration of hydrocolloids in the BS, among others, affect the dependent variables (DV) of the agglomerated powder: moisture content (Xw), water activity, apparent density (ρ_a), Carr index, Hausner ratio, solubility (S), wettability (*We*), dispersibility, angle of repose, particle size, total phenols (TP), radical scavenging, active components, yield, among others. The selection of the IVs depends on the level of automation of the equipment used, and the utilization of the response surface methodology 3(RMS) is convenient for investigations for the industry since it allows to improve their processes by providing a better understanding of the influence of the IVs on the DV of the powder matrix. The FBA process improves the techno-functional properties of fine powders, being of great application in the pharmaceutical, chemical and food industries; furthermore, agglomerated powders are convenient for preservation, transportation, storage, and processing [8]. In the food industry, its applications are found in a wide variety of products: fruit drinks, coffee, powdered milk and baby formulas, additives, artificial sweeteners, spices, colourants, proteins, cereals, flours, among others [9], with granule sizes ranging from microscopic to macroscopic sizes [10]. The literature does not contain any reports on FBA processes in blackberries, the agglomeration of lactose powder with a lactose solution as a binder is highlighted, where the authors highlighted the improvement in fluidity and compressibility when the size was more significant than 140 μm [11]; in concentrated rice protein powder using glucomannan as a BS, an agglomerated powder with low Xw, short t and improved fluidity was obtained [12]; in carotenoid-rich carrot concentrate powder, high encapsulation efficiency, oxidation stability and improved fluidity are highlighted [13]; in powdered agglomerated pectin, a more porous and irregular system is reported, with an improvement in its appearance, fluidity, *We* and S [14].

In this context, the research objective was to experimentally optimize the fluidized bed agglomeration (FBA) process of a blackberry powder mixture (ABPM) utilizing the response surface methodology.

2. Materials and methods

2.1. Experimental material

A blackberry powder mixture (BPM) obtained in an industrial SD (Lemar, China, model LPG320) was used as experimental material. The feeding consisted of blackberry concentrate, maltodextrin (MD) and gum arabic (GA) and the SD process was carried out under vacuum pressure, inlet air temperature: 159.3 °C, outlet air temperature: 89.3 °C and atomizing disc speed: 15000 rpm. The development of feeding and the conditions of the SD process at the pilot level have been described by De los Rios-Carvajal et al. [15] and Cortes-Rodriguez et al. [16]. For the industrial process, only the speed of the atomizing disc was modified, determining it from the same tangential speed of the pilot operation.

2.2. Agglomeration process

A fluidized bed encapsulator agglomerator (Changzhou Zhiyang Machinery Equipment Co, Ltd., reference DLP 1.5) was used, operating with a load of 350 g/batch. The BS was formulated with water and vitamin C (Vit. C), with the objective, the ABPM reached 30% of the daily reference value of nutrients - needs (NRV-N) in a portion of 30 g of ABPM, according to the Colombian regulations [17]. The process evaluation employed the response surface methodology, utilizing a central design comprising the central face ($\alpha = 1$) (15 experiments), considering the IV: T (50–70 °C), BS atomization air pressure (P) (1–2 bar) and t (20–35 min) (the minimum and maximum values were established according to previous tests), and the DV: Xw, S, *We*, ρ_a, TP, radical scavenging (ABTS·+ and DPPH·), Ant, ellagic acid (EA) and Vit. C. On the other hand, the BS flow was constant (1.3 mL/min) during t, determining the total volume to be incorporated (26.00–45.75 mL), with the BS mass/charge mass ratio between 0.07 and 0.13 kg/kg.

2.3. Physicochemical and physical characterization of BPM and ABPM

Moisture content (Xw): It was determined using the gravimetric method in a controlled-temperature oven (105 °C) until the sample reached a constant value (AOAC Official Method, 925.10) [18]. S: S was measured according to Cano-Chauca et al. [19] with some modifications. Specifically, 0.5 g of powder sample was stirred in 50 mL of water using a vortex mixer for 5 min. The suspension was then centrifuged at 3000 rpm for 10 min. An aliquot of the supernatant was transferred to a pre-weighed Petri dish and dried in an oven until reaching a constant weight. The soluble material was determined by the weight difference, and S was represented as a percentage. Wettability (*We)*: It was determined by measuring the time required for 0.1 g of sample to fully penetrate the surface of 100 mL of water at 25 °C [20]. Briefly, 0.1 g of the sample was scattered across the surface of 100 mL of water at 25 °C without agitation. The time required for the particles to become completely wet was recorded. ρ_a: the apparent density was determined according to Pereira et al. [21] with some variations. The sample (5 g) was placed into 10 mL Falcon tubes, and the volume occupied was determined; ρ_a was

calculated as the ratio of the weight and the volume of the sample. To determine the functional activity of the active components, methanolic extracts were initially obtained, where 0.1 g of sample was extracted with 40 mL of the methanol/water mixture (70/30). TP: Folin-Ciocalteu colorimetric method described by Da Silva et al. [22] was modified as follows: 100 μL of the extract and 400 μL of the aqueous solution of Na_2CO_3 (7.44% w/v) were mixed in Eppendorf tubes; the mixture was stirred in a vortex at 2000 rpm for 1 min and left to stand for 5 min; subsequently, 500 μL of Folin-Ciocalteu reagent (0.2 N) was added. The mixture was shaken and kept in the dark for 2 h; Subsequently, the absorbance at 760 nm was recorded using a Thermo Scientific Evolution 60 UV/VIS spectrophotometer. ABTS·+ radical scavenging: the ABTS·+ assay was conducted as described by Fang et al. [23]. The ABTS·+ cation radical was obtained by reacting an ABTS·+ solution (2,2′-azino-bis-(3-ethylbenzothiazoline)-6-sulfonic acid) (7 mM) with potassium persulfate (2.45 mM) (1:1 ratio) in the absence of light at 25 °C for 16h; then, it was diluted in ethanol until reaching an absorbance 0.70 at 754 nm. Next, an aliquot of 950 μL of the ABTS·+ solution was combined with 50 μL of the methanolic extract. The mixture was vortexed at 2000 rpm for 1 min and then kept in the dark at 25 °C for 7 min; finally, the absorbance reading was made at 734 nm. DPPH· radical scavenging: the methodology described by Rodríguez-Gutiérrez et al. [24], was employed. A working solution of DPPH· 0.025 Mm with an absorbance of 0.70 at 517 nm was prepared from a 3.19 mM methanolic solution of DPPH· (6-hydroxy-2, 5,7, 8-tetramethylchromane-2-carboxylic acid 97%). A total of 950 μL of DPPH· solution and 50 μL of the methanolic extract were mixed in Eppendorf tubes, vortexed at 2000 rpm for 30 s and left to react in the dark at 25 °C for 30 min. The absorbance at 517 nm was determined.

Ant and EA: The extracts were prepared from 250 g of sample and according to the methodology described by Cortes-Rodriguez et al. [16]. Similarly, the quantification of C_3G and EA was performed by HPLC (Prominence 20A, Shimadzu, Japan) with a DAD-UV-VIS detector (200–700 nm) and according to the methodology described by Cortes et al., 2022. Vit. C: 0.25 g of sample was introduced into a graduated test tube, and added to the mixture was a buffer solution of 0.02 M KH_2PO_4, which had been adjusted to pH 3.0 using 85% orthophosphoric acid, up to 20 mL. The mixture was stirred for 2 min in a vortex, centrifuged at 5000 rpm (4 °C and 15 min); the supernatant was filtered through a 0.45 μm acetate-cellulose membrane and placed in an amber vial. Quantification was performed by HPLC (Shimatzu Prominence 20A) equipped with a Luna® C18(2) column (5 μm, 100 A, 250 × 4.6 mm), mobile phase: KH_2PO_4 0.02 M − pH: 3.06, flow: 1 mL/min, pressure: 1172 psi, retention times: 4.37 min, injection volume: 5 μL and wavelength: 244 nm. The analytical standard was L-Ascorbic acid (Sigma Aldrich 47863, Lot LRAC1812).

2.4. BPM and ABPM morphology

A scanning electron microscope (SEM) (JSM-5910, JEOL) was used, operating the equipment with a high vacuum, and coating the

Table 1
Results of the dependent variables of the ABPM according to the experimental design of the agglomeration process.

Run	T (°C)	t (min)	P (Bar)	X_w (%)	S (%)	$\underline{W_e}$ (min)	ρ_a (g/mL)	TP (mg GAE/100 g db)	ABTS·+ (mg TE/100 g db)	DPPH· (mg TE/100 g db)	Ant (mg C_3G/100 g db)	EA (mg/100 g db)	Vit. C (mg/100 g db)
1	60	27.5	1.5	9.6 ± 0.1	78.5 ± 1.1	10.2 ± 1.1	0.352 ± 0.479	3872.6 ± 66.3	4042.9 ± 119.1	5315.2 ± 192.3	123.1 ± 5.8	1950.5 ± 136.7	28.2 ± 3.2
2	70	35.0	1.0	7.6 ± 0.1	80.2 ± 0.2	16.3 ± 1.0	0.377 ± 0.395	3719.1 ± 24.8	3954.0 ± 65.9	4649.2 ± 117.3	139.0 ± 6.8	2077.4 ± 22.1	30.5 ± 3.7
3	60	27.5	1.5	8.8 ± 0.4	76.5 ± 1.1	9.9 ± 0.0	0.384 ± 0.44	3779.8 ± 33.5	3891.3 ± 53.1	5745.0 ± 223.7	130.9 ± 3.5	1926.1 ± 24.5	29.2 ± 2
4	60	27.5	1.0	9.5 ± 0.0	78.5 ± 0.7	20.6 ± 1.6	0.413 ± 0.444	3996.7 ± 95.2	3706.1 ± 135.8	5881.4 ± 244.9	133.7 ± 2.2	1993.4 ± 13.1	21.9 ± 0.4
5	70	27.5	1.5	8.7 ± 0.2	83.7 ± 0.2	22.5 ± 0.5	0.356 ± 0.397	3668.3 ± 2.2	4461.7 ± 137.8	5209.1 ± 90.6	151.5 ± 2.2	2322.0 ± 81.6	36.2 ± 3.1
6	70	20.0	2.0	8.3 ± 0.1	82.2 ± 0.2	23.1 ± 0.5	0.368 ± 0.396	3857.2 ± 23.6	4399.0 ± 77.1	5846.6 ± 156.5	152.1 ± 3.8	2022.5 ± 25.4	28.9 ± 0.4
7	60	35.0	1.5	9.1 ± 0.1	80.9 ± 0.6	27.1 ± 0.8	0.376 ± 0.413	3058.8 ± 27.1	4900.5 ± 78.5	5397.0 ± 281.9	133.8 ± 3.7	2152.4 ± 8.3	16.7 ± 8.2
8	60	20.0	1.5	8.1 ± 0.1	81.4 ± 1.4	16.4 ± 1.2	0.380 ± 0.408	4492.4 ± 35.1	4900.5 ± 79.3	5397 ± 158.3	145.1 ± 9.3	2290 ± 196.1	35.1 ± 8.2
9	60	27.5	1.5	8.5 ± 0.1	77.1 ± 0.4	10.6 ± 0.7	0.400 ± 0.440	3755.4 ± 33.7	4070.4 ± 84.3	4820.4 ± 143.3	138.0 ± 4.8	2050 ± 129.0	26.5 ± 0.6
10	60	27.5	2.0	9.0 ± 0.0	78.1 ± 0.4	14.3 ± 2.0	0.368 ± 0.427	3757.0 ± 5.6	4690.9 ± 55.2	5100.4 ± 48.6	142.9 ± 1.9	1965.4 ± 14.0	24.8 ± 0.7
11	60	27.5	1.5	8.8 ± 0.1	78.2 ± 0.6	10.6 ± 2.6	0.376 ± 0.44	3860.6 ± 68.8	4894.4 ± 100.5	5511.3 ± 143.7	131.6 ± 9.8	1890.5 ± 35.4	27.0 ± 15.0
12	50	35.0	2.0	11.1 ± 0.3	77.6 ± 1.3	5.1 ± 0.4	0.349 ± 0.476	4028.7 ± 38.1	5168.8 ± 230.9	5054.8 ± 16.9	139.3 ± 4.5	2195.1 ± 21.3	23.6 ± 17.1
13	50	20.0	1.0	9.3 ± 0.2	81.0 ± 1.2	11.5 ± 0.5	0.377 ± 0.413	4682.4 ± 54.9	4851.7 ± 212.4	5276.1 ± 269.3	148.0 ± 0.3	2113.9 ± 84.4	43.9 ± 16.9
14	50	27.5	1.5	9.2 ± 0	81.5 ± 0.9	16.8 ± 1.7	0.343 ± 0.391	3966.1 ± 27.1	4737.6 ± 52.6	6527.6 ± 258.2	146.7 ± 7.3	2157.1 ± 38.5	39.3 ± 13.9
15	60	27.5	1.5	9.0 ± 0.1	78.0 ± 1.4	10.9 ± 0.6	0.379 ± 0.411	3732.9 ± 87.9	4863.1 ± 48.4	4882.9 ± 132.4	132.2 ± 5.4	2060.3 ± 20.8	28.0 ± 2.0

samples with gold. The analysis of the micrographs was conducted using an acceleration voltage of 10 kV and with a scale of 100, 300, 600 and 1000 magnifications [25].

2.5. Statistical analysis

The data obtained was statistically analyzed using ANOVA, with a significance level of 95% ($\alpha = 0.05$), using the Statgraphics Centurion XVII software (version 17.2.00/2016). The DV (3 repetitions/experiment) were modelled using a second-order polynomial equation with three repetitions per experiment (equation (1)), where Y: DV, β_0: constant, β_A, β_B, and β_C: coefficients of the IV A, B and C respectively; β_{AB}, β_{AC}, and β_{BC}: interaction coefficients of linear variables; and β_A^2, β_B^2 and β_C^2: coefficients of the quadratic interactions. The models were adjusted according to the lack of fit method and the regression coefficient (R^2). At the same time, the process conditions that reflected the most satisfactory quality attributes in the ABPM were obtained from an experimental optimization of numerous responses, defining criteria, and results for each DV. On the other hand, a validation of the mathematical model was carried out based on the proximate mean error (RME), comparing the values predicted by the model and the experimental values at the optimal condition (3 replicates) (Equation (2)).

$$Y = \beta_0 + \beta_A A + \beta_B B + \beta_C C + \beta_{AB} AB + \beta_{AC} AC + \beta_{BC} BC + \beta_{A^2} A^2 + \beta_{B^2} B^2 + \beta_{C^2} C^2 \quad (1)$$

$$RME = \left| \frac{\text{Model value} - \textit{Experimental} \text{ value}}{\textit{Model value}} \right| \text{x } 100 \quad (2)$$

3. Results and discussion

The properties of the BPM were the following: Xw = 6.0 ± 0.1%, S = 79.6 ± 0.2%, *We* = 120.3 ± 2.0 min, ρ_a = 0.352 ± 0.006 g/mL, TP = 4459.7 ± 20.4 mg gallic acid equivalent (GAE)/100 g db, radical scavenging: ABTS·+ = 4900.9 ± 82.3 mg Trolox equivalent (TE)/100 g db and DPPH· = 5105.1 ± 44.3 mg TE/100 g b, Ant = 159.3 ± 14.9 mg C_3G/100 g db, EA = 2047.8 ± 95.6 mg/100 g db and Vit. C = 22.3 ± 1.6 mg/100 g db. Preliminary tests identified problems with the fluidisation of the BPM by forming thick agglomerate complexes in the air distributor and areas of accumulation of granulated product that was not suspended in the bed, generating instability in the process. This problem was corrected by mixing the BPM with Pirosil PS-200 (Glassven Yangzhong Additives JV Ltd.) at 1%. Table 1 shows the mean values and the standard deviation of the DV of the ABPM.

3.1. Moisture content

In the agglomeration method, the Xw experienced changes in the mean values between 7.6 and 11.1%; however, the ANOVA showed no significant statistical differences ($p > 0.05$) regarding the IV or their linear quadratic interactions. This situation suggests that the surface adsorption of the BS on the filler material particles occurs randomly without describing a well-defined trend of the effect of the IV. Therefore, it confers these ranges of variation, being in all the experiments the Xw of the ABPM > BPM (6.02 ± 0.10%). This condition denotes a food with a level of Xw close to the moisture content of the monolayer, which could guarantee physicochemical stability during storage [26].

Fig. 1 represents the graph of the response volume of the Xw of the ABPM, observing that the lowest values of Xw (blue zone) (> bond strength between the particles) are found when the system operates at 1) high T (68–70 °C), t (32–35 min) and P (1.0–1.4 bar), and 2) T (50–66 °C), t (20–23 min) and P (1.5–2.0 bar). The first condition corresponds to the most significant driving force for heat transfer that favours the most excellent mass transfer during evaporation [27], but with higher water contents at the liquid junction points between the particles, given the lower BS atomization pressure [28]; while the second condition could be occurring due to lower water content at the liquid junction points, which requires less driving force for mass transfer (low t and T).

Fluctuating values of Xw have been reported by various authors in agglomerated food matrices: isolated pea protein (6.94–9.35%)

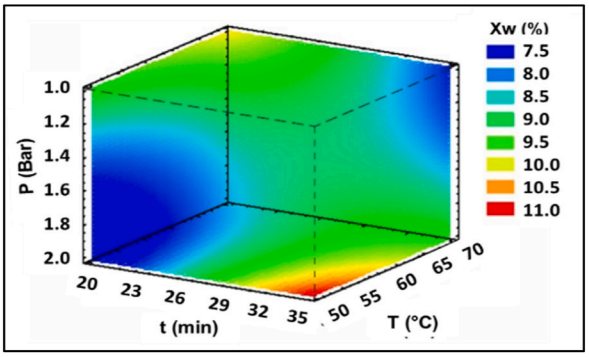

Fig. 1. Response volume graph of the Xw of the ABPM. Xw: moisture and ABPM: agglomerated blackberry powder mixture.

[29] and concentrated rice protein using a collagen hydrolysate as BS (4.12 and 3.10%) [30] and 4.15% [31]; also in other products: microcrystalline cellulose using a water-soluble polyvinylpyrrolidone binder solution (Xw < 5%) [32].

3.2. Properties associated with the reconstitution of ABPM

The S, *We* and ρa are physical properties that undergo structural modifications during the agglomeration process; so, they are closely related to the IV of the process and are reflected on the properties of instantaneity, fluidity, and release of active ingredients of the powders [33]; In addition, the reconstitution in the water of the agglomerated products depends on the pH and dissolution temperature [34]. On the other hand, reconstitution involves 4 phases: penetration of the liquid into the pore spaces of the matrix, sinking of particles and the process involves the dispersal of the powder in the liquid and the potential dissolution of the particles (if the substance is soluble) [35].

The mean values of the S of the ABPM fluctuated according to the combinations of the experimental design between 76.5 and 83.7%, highlighting that the values were lower than the values found for the BPM (88.01 ± 0.17%), which is attributed mainly to the presence of silicon dioxide in the ABPM, which has a low S in water (0.012 g/100 g) [36]; and additionally, to the insoluble material from the BPM. Now, microstructurally, these materials could be located on the surface, contributing to the lower S than the BPM. The ANOVA presented significant statistical differences ($p < 0.05$) of the S for the quadratic interactions T-T and P–P. Fig. 2 indicates the surface and volume graphs representing the S response for the ABPM, identifying the quadratic interactions in the curvilinear behaviour of T and P. Convex curves for P are observed that describe maximum values of S (yellow zone) at T high (70–66 °C) and with operating P between 1.4 and 1.8 bar; in addition, concave curves for T that describe minimum points of S (blue zone) at high P (1.9–2.9 bar) (Fig. 2A), not favourable for the product, between 52 and 58 °C. The response volume graph describes in the three-dimensional plane the most favourable conditions of the S during the agglomeration process (yellow-red zone): T (68–70 °C), P (1.2–2.0 bar) and throughout the range of t (Fig. 2B).

The mean values of the *We* of the ABPM fluctuated between 5.1 and 27.1 min, highlighting positively a significant decrease for the BPM (120.3 ± 2.0 min), which is attributed to the greater diffusion experienced by the water inside the ABPM, being moistened in a shorter time, given the porous microstructure and the larger particle size conferred during the FBA process. However, the results obtained could be considered high; probably still, the surface exhibits a reduced capacity for absorbing reconstitution water via capillary forces [37]. The ANOVA identified *We* as a critical variable since it presented significant differences ($p < 0.05$) for all the IV and their linear and quadratic interactions. Fig. 3 presents the graphs of main effects, surface, and response volume of the *We* of the ABPM. It is observed in the graph of main effects that the IV t and T have a directly proportional effect with the *We*, whereas the P is inversely proportional (Fig. 3A). The response surface graphs illustrate the zones where the t-T, T-P and P-t interactions favour the lowest values of *We* (blue zone) (Fig. 3B, C and 3D), described when the system operates at t (20–23 min), T (50–54 °C) and P (2.0–1.8 bar), which is confirmed in the response volume graph (Fig. 3E), where the most favourable operating conditions were: t (20–23 min), T (50–56 °C) and P (2.0–1.6 bar).

In general, the results obtained show that the agglomeration process improves the rehydration properties for what was found at BPM, suggesting a higher capability to counteract surface tension at the solid-liquid interface, and therefore facilitate that ABPM is wet faster [38]; on the other hand, there is a synergistic effect with the composition of ABPM, which are mainly made up of carbohydrates and polar molecules such as An, organic acids, vitamins, among others [39], which favour the dissolution of solid bridges between particles [40]. The literature does not report investigations in berry-type fruits in agglomerated food products. The work carried out by Atalar et al. [41] in agglomerated powder of commercial yoghurts, who reported S values of 55% and a decrease in *We* for the load material (2 h → 7–8 s); in addition, by Atalar et al. [42], who reported for the agglomerated powder of the fungus (*Agaricus bisporus*): a decrease in *We* from values > 1 h → 3.75–22.5 s and an increase in S 21 0.6 → 27.6%).

On the other hand, in powdered food products, the research carried out by De Farias et al. [31] stands out, who reported a decrease in *We* (140 → 40) for concentrated rice protein; and by Barkouti et al. (2013) [9], who reported for skim and whole milk, a decrease in *We* from times >1 h → 4 s and times >2 h → 29 s, respectively. On the other hand, not so favourable effects were reported in whey protein powders, showing low wetting behaviour (*We* > 20 min) [34].

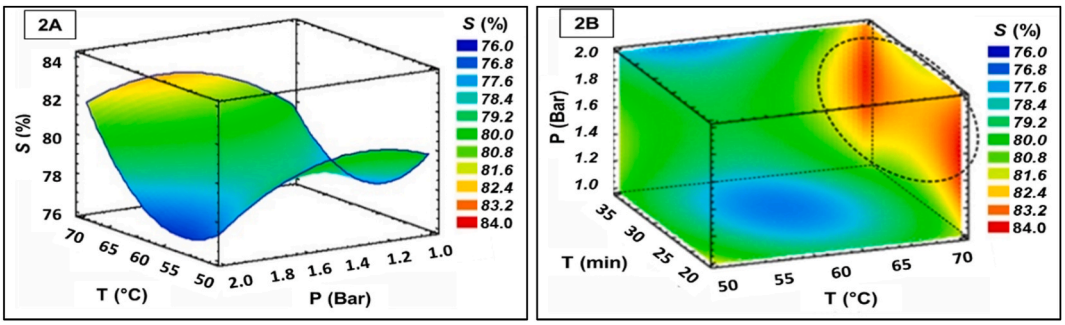

Fig. 2. Response surface and volume graphs of the S of the ABPM. S: solubility and ABPM: agglomerated blackberry powder mix.

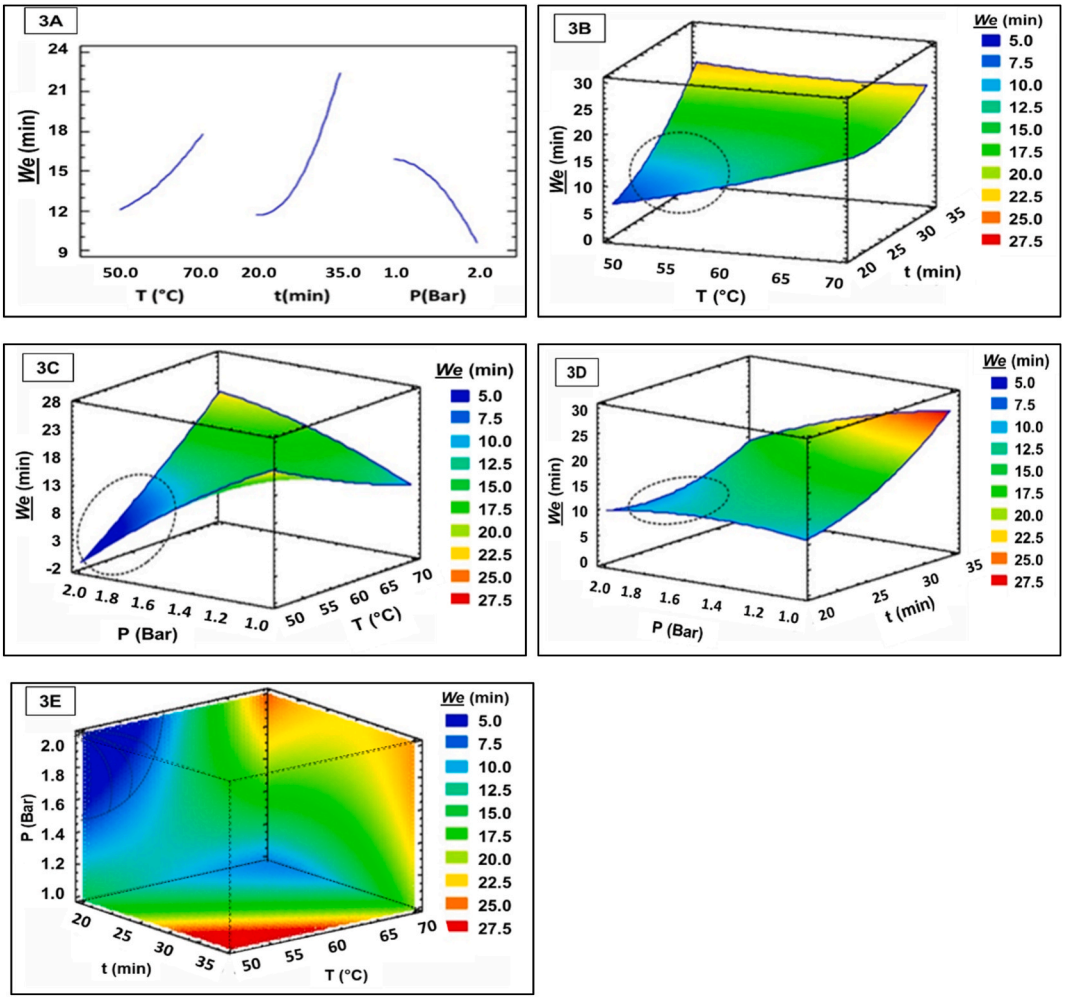

Fig. 3. Main effects graph and response surface and volume graphs of the *We* of the ABPM. *We*: Wettability and ABPM: agglomerated blackberry powder mixture.

3.3. Apparent density

The mean values of the ρ_a of the ABPM fluctuated between 0.343 and 0.413 g/mL, being in some cases higher or lower than the values found in the BPM (0.352 ± 0.006 g/mL). The variability of ρa in the ABPM does not describe a well-defined trend of the influence of the IV evaluated, which was corresponding to the results of the ANOVA, as there were no significant differences in ρ_a ($p > 0.05$) for to the IV, and the linear and quadratic interactions did not show any significant impact. This situation suggests that the

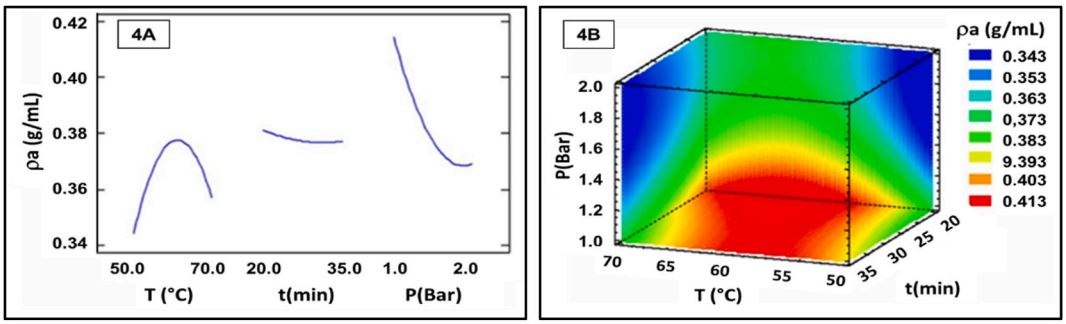

Fig. 4. Main effects and response volume of the ρ_a of the ABPM. ρa: apparent density and ABPM: agglomerated blackberry powder mix.

agglomeration process can confer greater or lesser densification of the material, probably depending on different phenomenologies: 1) an increase in density due to the increase in Xw of the agglomerated matrix, 2) an increase in interporosity particle (volume fraction of the internal cavities), the shape and size of the particles, due to the same agglomeration process, 3) a possible volumetric contraction during t, due to thermal stress, 4) changes in the cohesive forces ABPM, among others.

Various behaviours of ρ_a have been reported in different agglomerated food materials: 1) Lee et al. [43] reported changes in ρa in xanthan gum powder (0.35, 0.39, 0.38, 0.37 g/mL) due to the effect of BS: glucose, lactose, sucrose and sorbitol, respectively; 2) Lee et al. [44] reported in guar gum and locust bean agglomerated powders, ρ_a values that fluctuated between (0.25–0.54 g/cm^3) and

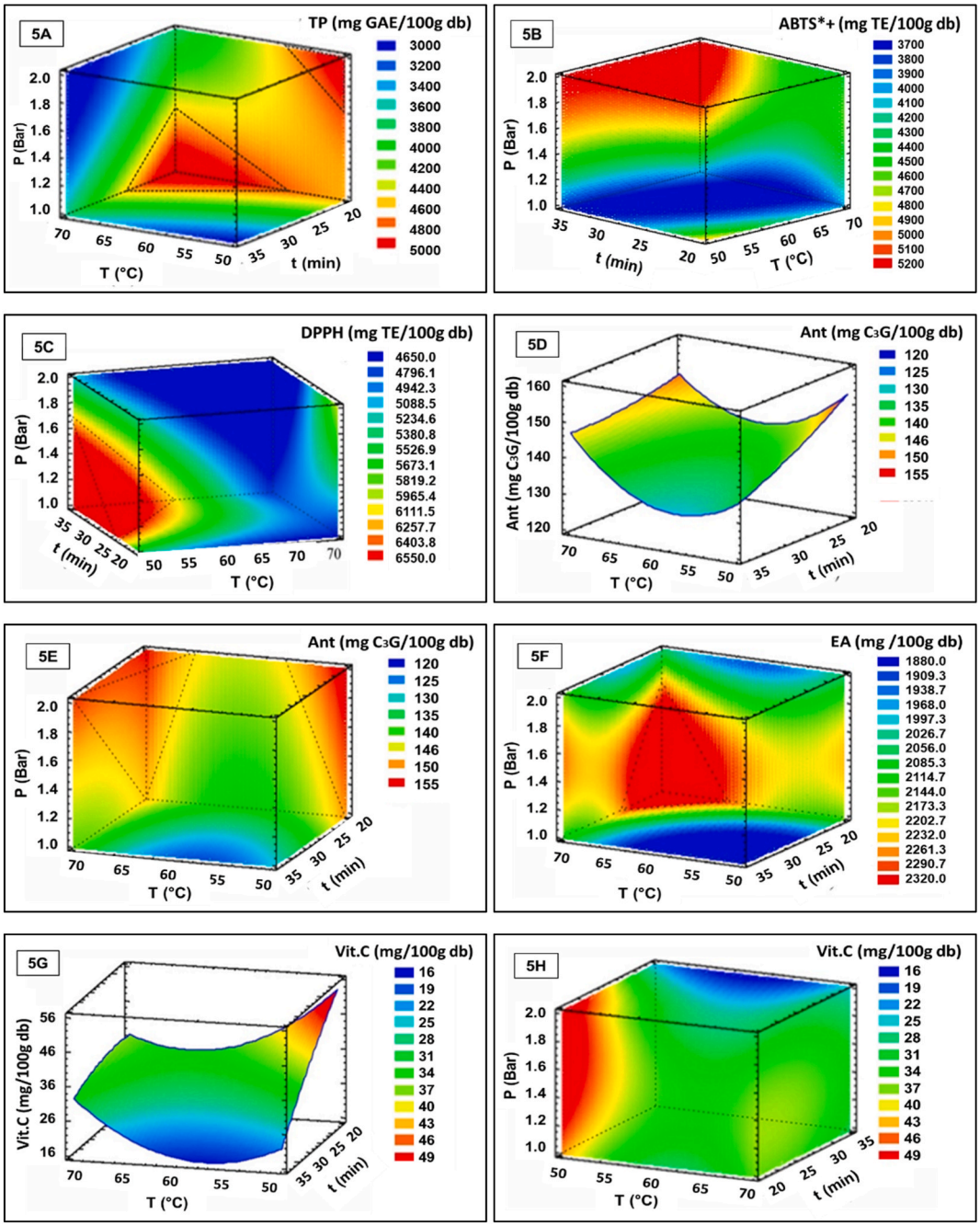

Fig. 5. Response surface and volume graphs of the TP (Fig. 5A), antioxidant capacity (ABTS*+: Fig. 5B and DPPH: Fig. 5C) and active components (Ant: Fig. 5D and E, EA: Fig. 5F, and Vit.C: Fig. 5G and H) of the ABPM. TP: total phenols, ABTS·+: 2,2′-azinobis-(3-ethylbenzothiazoline-6-sulphonate) radical, DPPH·: 2,2-diphenyl -1-picrylhidrazyl radical, Ant: Anthocyanins, EA: ellagic acid, Vit. C: vitamin C and ABPM: Agglomerated blackberry powder mix.

(0.32–0.56 g/cm^3) respectively; 3) Yuksel et al. [45] informed the production of agglomerated spinach powder using various binding solutions BS (MD, GA and whey protein isolate), values of 561, 437 and 243 kg/m^3, respectively; 4) Benelli et al. [46] reported on microcrystalline cellulose powder using different BS (GA and whey protein concentrate), ρ_a values (0.80 and 0.76 g/mL), respectively; and 5) Jeong et al. [47] reported xanthan gum agglomerated powder using a BS of hydroxypropyl methylcellulose (0–6%), ρa values between 0.44 and 0.76 g/mL, respectively. Fig. 4 presents the main effects graph and the response volume graph of the ρa of the ABPM. The main effects plot (Fig. 4A) suggests a more significant influence on changes in the ρa of the IV T and P; meanwhile, the response volume graph (Fig. 4B) allows to identify of two regions where ρa becomes smaller (blue area), which directs to an advance in the instantaneous effects: 1) T (68–70 °C), P (1, 4–2.0 bar) y t (20–23 min); 2) T (54–50 °C), P (1.4–2.0 bar) y t (32–35 min).

In both conditions, the P was similar and over high values, which suggests better spraying and impregnation of the BS on the surface of the particles; however, in the first process condition, the high T could be generating more compact agglomerates with lower Xw content, decreasing the ρa and thus increasing the functionality in the *We* [48–50]. In the second process condition, the lower T are offset by, the higher t's, contributing to a similar microstructure.

3.4. Total phenols, radical scavenging, and active components of ABPM

The mean values of TP content and radical scavenging (ABTS·+ and DPPH·) of ABPM varied between (3058.6–4682.4 GAE/100 g db), ABTS·+ (3706.1–5168.8 mg TE/100 g db), DPPH· (4649.2–6527.6 mg TE/100 g db) respectively, where the ANOVA showed that the TP presented statistically significant differences ($p < 0.05$) for T, t and with the T-P and P–P interactions. On the other hand, ABTS·+ and DPPH· did not show significant differences ($p > 0.05$) with any IV or their linear and quadratic interactions. On the other hand, the mean values of the content of Ant, EA and Vit. C of the ABPM fluctuated between (123.1–152.1 mg C_3G/100 g db), (1890.5–2322.0 mg/100 g db) and (16.7–43.9 mg/100 g db) respectively, the latter corresponding to a variation of 20.1–52.9% NRV-N/100 g db respectively. The ANOVA presented significant differences in the content of Ant and EA for the quadratic interactions of the T and P, respectively, while Vit. C was the variable most sensitive to the IV, presenting significant differences for t and the interactions T-t, T-P, T-T and P–P.

Furthermore, moderate ($0.2 < r < 0.5$) to low ($r < 0.2$) Pearson correlations were found between the secondary metabolites (TP, Ant, EA and Vit. C), quantified in the agglomerated blackberry powder mix, and the radical scavenging values obtained. This fact suggests that there is some but not a strong relationship between the secondary metabolites and the radical scavenging of ABPM. Finally, the comparison of the results obtained from the ABPM for the BPM obtained by SD and used as raw material is highlighted: TP (4459.7 ± 20.4 GAE/100 g db), ABTS·+ (4900.9 ± 82.3 mg TE/100 g db) and DPPH· (5105.1 ± 44.3 mg TE/100 g db), Ant (159.3 ± 14.9 mg C_3G/100 g db), EA (2047.8 ± 95.6 mg/100 g db) and Vit. C (22.3 ± 1.6 mg/100 g db).

Fig. 5 presents the graphs of surface and volume response of the TP, the radical scavenging, and the active components of the ABPM. It is observed that the TP content (Fig. 5A) is enhanced when the system works at two process conditions: 1) low t (20–25 min), low P (1.0–1.4 bar) and T (62–70 °C), and 2) low t (20–23 min), low P (1.7–2.0 bar) and T (50–54 °C). In general, a more significant conservation of TP is noted at low t, being mainly synergistic at low T, where its content in ABPM is maximized. Regarding the ABTS·+ (Fig. 5B) and DPPH· (Fig. 5C), the best-operating conditions were: [t (32–35 min), P (1.6–2.0 bar) and throughout the range of T] and [t (32–35 min), P (1.0–1.5 bar) and T (50–56 °C)] respectively, which denotes a different behaviour in the agglomeration process. The scientific literature is incipient in research work on agglomerated food products; therefore, the results obtained confer an added value to the present investigation. The data reported by Farias-Cervantes et al. [51] in microencapsulated by SD for blackberry powder *Rubus adenotrichos* L. and *Rubus fruticosus* L with DPPH· values of 6.2 and 4.4 mg TE/100g, respectively, and ABTS·+ of 406.2 and 379.8 mg TE/100 g, respectively. Horszwald, Julien and Andlauer (2013) [52], aronia berry powder TP: 34.8 mg GAE/100 mg, ABTS·+ 251.34 and DPPH· 26.49 μmol TE/100 mg [50].

Regarding the content of Ant (Fig. 5D and E), it presented a curvilinear behaviour (convex curve) for T, illustrating minimum values at T between 54 and 58 °C; in contrast, the response volume plot illustrated two zones where higher Ant content is favoured: 1) high T (68–70 °C), t (20–29 min) and P across the range; and 2) low T (50–52 °C), low t (20–22 min) and P throughout the scope. For the EA content (Fig. 5F), there is a well-defined zone where higher contents were observed: high T (62–70 °C), t (20–25 min) and P (1.0–1.6 bar). In SD processes, Santos et al. [53] found in blackberry powder concentrations of Ant: 811.85 mg C_3G/100 g and EA 702.61 mg/100 g. Strawberry powder Ant: 542.7 mg total anthocyanins/100 g db and EA 32.3 mg/100 g db [54]. In EA moringa powders: 33.4 μg/g [55].

Vit. C (Fig. 5G and H) was the most sensitive variable to the agglomeration process, where its greatest degradation occurs at higher t; however, the t-T interaction is favoured when these properties are low, which corresponds to lower thermal stress [56]. On the other hand, the T-P interaction revalidates a potentiation of the Vit. C content. Low content of Vit. C to high values of T and P, where a more significant number of sprayed droplets of SL containing Vit. C moisten a more significant number of fine particles of ABPM, increasing the liquid bridges, the size of the agglomerate and the cohesion forces, acting the system with a protective effect of Vit. C and the present active components [42,44]. Finally, the response volume plot summarizes the most favourable Vit. C conditions: low T (50–52 °C), low t (20–22 min), and P across the range. Vit. C is characterized by being a labile component, and its degradation depends on factors that include the presence of temperature, light, moisture content, O_2, pH, oxidizing agents, among others [57].

Some investigations have evaluated the effect of the agglomeration process on other active components. Rayo et al. [25] reported that in the manufacturing of instant green banana flour, the process did not affect its chemical structure; on the other hand, Dłuzewska et al. [58] evaluated the retention of β-carotene using different encapsulants (GA, MD, modified starch and whey protein), finding a decrease of approximately 50%; furthermore, that the walls of the microcapsules, formed with GA and MD provided better protection against degradation. On the other hand, Nogueira et al. [59] reported that, during the SD process, the encapsulating agents could

protect Vit. C from thermal degradation and oxidation, retaining 90.8% compared to the fruit in the fresh state (134.6–194.7 mg/100 g), with Vit. C values: 285.7 mg/100 g. On the other hand, Sadowska et al. [54] reported 3.2 ± 0.2 mg Vit. C/g db for strawberry powder.

In general, it is considered that the lower values obtained for TP, radical scavenging and active components in ABPM are a consequence of the sum of various factors, mainly due to: 1) the presence of total solids provided by proxy; 2) the presence of higher water content in the food matrix; and 3) effects of thermal degradation, high T and t, during the agglomeration process [60]; while, the higher values could be favoured by: 1) the higher active components content in the raw material; 2) by the porous microstructure of the ABPM, which facilitates the extraction of these active components; 3) by the protective effect of the encapsulants (MD and GA) against deterioration reactions due to the effect of thermal stress; and 4) due to the low T and t of the process [61,62]. On the other hand, Dacanal et al. [63] suggest that AC fluctuations could also be associated with the fluidisation process, with the dissipation of kinetic energy between the particles and the internal wall of the chamber, with the speed of deformation, the content of Xw and the chemical composition of the particles.

3.5. Modelling and experimental optimization of ABPM

In general, the DV modelling described that the fluidized bed agglomeration process generated satisfactory results. The behaviour of Xw, TP and Vit are mainly highlighted. C, which presented greater precision ($R^2 > 92.5\%$); while S, ρa, ABTS·+, DPPH·, An, and EA presented R^2 values between 64.4 and 74.9% and the one with the slightest adjustment was $\underline{We}$ ($R^2 = 56.6\%$), given its great affectation by the independent variables considered. It is considered that the experimental data are explained, and the developed models showed a variation around the mean [64], adding that the lack of fit test identified that most of the DV (ρa, TP, ABTS·+, DPPH·, Ant and Vit. C) were not statistically significant ($p > 0.05$); In addition, all the DV presented a random distribution of the residuals, which allows us to ensure that the data can be adjusted according to a normal distribution.

According to the results obtained, the planning of experimental enhancement of numerous responses was carried out by setting criteria, weights and impacts that favoured the final quality of the ABPM (Table 2). The experimental optimization presented desirability of 80.0%, defining the optimal conditions of the IV as follows: T: 70 °C, t: 21.7 min and P 1.13 bar. The experimental validation of the mathematical models presented acceptable results, where 80% of the values of the DV had a good SMR (<20%), except for DPPH· and Ant (24.0 and 44.7%, respectively).

3.6. Particle micrographs

The morphology of the BPM and ABPM obtained at the optimal condition were visualized using SEM, as shown in Fig. 6. The micrographs at scales 100, 300, 600 and 1000 magnifications identify the BPM (column 6A) as fine particles and smaller than the ABPM, with a smooth, spherical surface and somewhat collapsed because of the rapid water evaporation during the SD process. In addition, minimal agglomeration is observed despite having low levels of Xw, caused by the cohesiveness of its components (sugars such as sucrose, glucose, and fructose, along with organic acids like malic and citric acid). On the other hand, the ABPM (column 6B) presents a porous, irregular, rough, collapsed, and agglomerated microstructure of larger size, caused during the fluidisation process, where the particles wetted with the BS collide with each other initially forming agglomerates of small to medium through liquid bridges. Subsequently, the association of the agglomerated structures becomes consolidated and stabilized through the solid bridges during gentle drying at the T of air entry, conferring greater size and higher porosity (Andreola et al., 2018; Avilés-Avilés et al., 2015). This microstructural configuration allows a decrease of ρa and improves the wetting properties, which supports the good results of the $\underline{We}$ of ABPM (5.1 and 27.1 min) compared to those of the BPM (120.3 ± 2.0 min).

4. Conclusions

The response surface methodology was utilized to optimize multiple responses, and the experimental validation was conducted to verify that the obtained results were adequate for defining the operating parameters of the agglomeration process, presenting most of

Table 2
Experimental optimization of the ABPM agglomeration process.

Variable	Criterion	Impact	Weight	Experimental value	Theoric value	|EMR|* (%)
X_w (%)	Minimize	3	0.5	9.7 ± 0.1	9.5	1.68
S (%)	Maximize	5	1.5	74.9 ± 4.9	81.79	8.49
$\underline{W_e}$ (min)	Minimize	5	1.5	13.7 ± 3.6	11.42	19.86
ρ_a (g/mL)	Maximize	5	0.8	0.312 ± 0.009	0.393	20.00
TP (mg GAE/100 g db)	Maximize	4	0.8	4084.6 ± 30.6	4910.6	16.82
ABTS·+ (mg TE/100 g db)	Maximize	4	0.8	4511.4 ± 124.4	4005.9	12.62
DPPH· (mg TE/100 g db)	Maximize	4	0.8	4182.6 ± 66.4	4918.1	14.96
Ant (mg C_3G/100 g db)	Maximize	4	0.8	213.6 ± 15.9	147.6	44.67
EA (mg/100 g db)	Maximize	4	0.8	1878.2 ± 45.9	2471.3	24.0
Vit. C (mg/100 g db)	Maximize	5	1.2	29.8 ± 7.4	37.2	19.9
%VRN-N Vit. C/30g ABPM				9.7 ± 2.4	–	–

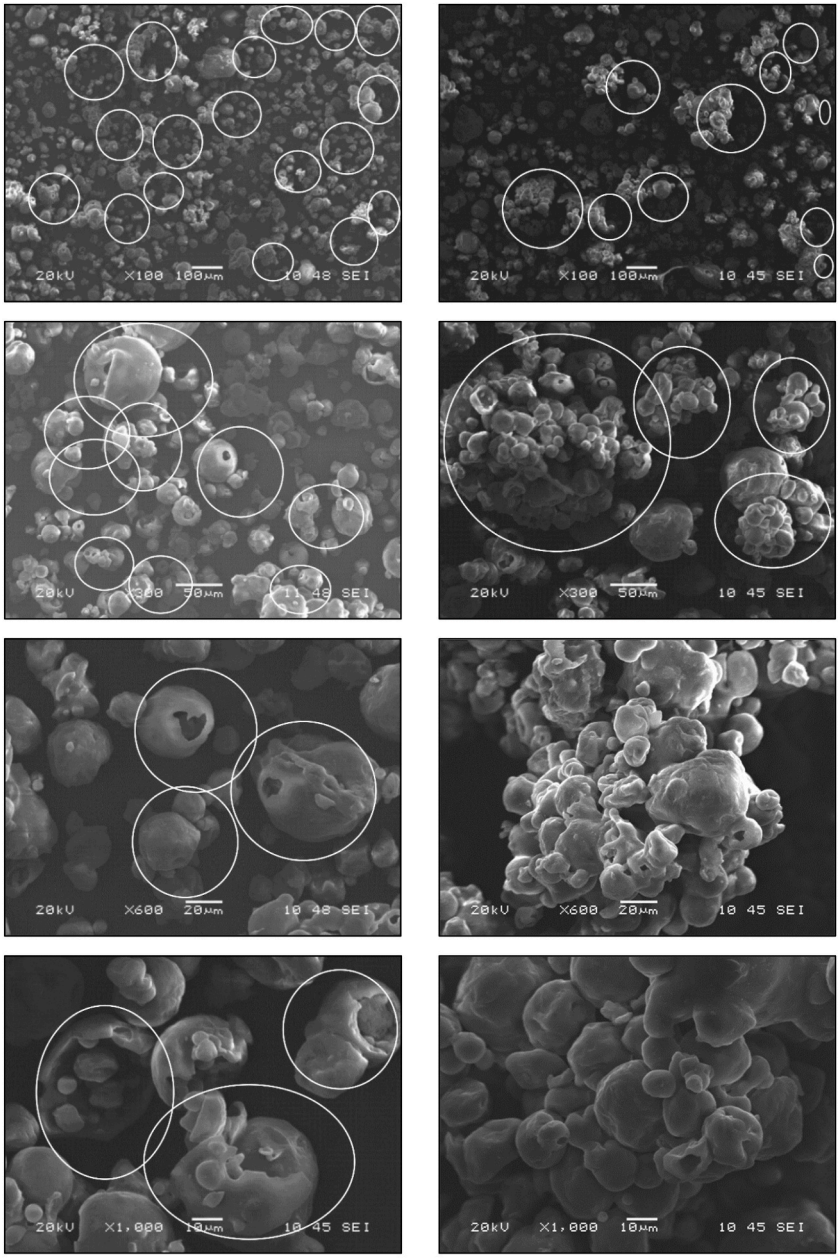

Fig. 6. Sem for BPM (column 6A) and ABPM (column 6B).

the mathematical models of the DV with good regression fits. Using a fluidizing agent such as pyroxyl improved the flow properties of the BPM, allowing adequate suspension of the bed during the process. The configuration of a larger, irregular, porous microstructural complex in the ABPMs contributed significantly to the decrease in their ρa and *We*, and, therefore, in the reconstitution properties. On the other hand, the active components of the ABPM are affected by the process conditions (mainly Vit. C). However, ABPM has a significant nutritional value due to its content of TP, Ant, EA and Vit. C, which give it good radical scavenging. It should be noted that a 30 g portion of ABPM makes it possible to prepare 250 mL of a drink with 11 °Brix and a contribution of approximately 10% of the NRV-R according to Colombian regulations. Few investigative works are reported on the use of agglomeration technology in fruits. However, this research offers positive results that encourage further progress in this field, in addition to being able to develop new raw materials or improved raw materials with potential use for the modern consumer, such as instant drinks or other types of home reconstitution food, and as raw material for the food industry.

Author contribution statement

Misael Cortés Rodríguez: Conceived and designed the experiments; Performed the experiments; A …

Data availability statement

Data will be made available on request.

Declaration of competing interest

The authors declare that they have no known competing financial interests or personal relationships that could have appeared to influence the work reported in this paper.

Acknowledgments

The authors thank the Secretary of Agriculture and Rural Development of the Department of Antioquia, Minciencias, and the Universidad Nacional de Colombia for financial support for this research project.

Abbreviations

Words	*Abbreviature*
Agglomerated blackberry powder mix	ABPM
Apparent density	ρa
Anthocyanins	Ant
Binder solution	BS
Binder solution atomization air pressure	P
Blackberry powder mix	BPM
Cyanidin-3-glucoside	C_3G
Ellagic acid	EA
Dry base	db
Dependent variables	DV
Fluidized bed agglomeration	FBA
Fluidizing air inlet temperature	T
Gallic acid equivalent	GAE

Words	*Abbreviature*
Glass transition temperature	Tg
Gum arabic	GA
Independent variables	IV
Maltodextrin	MD
Moisture	X_w
Processing time	t
Scanning electron microscope	SEM
Solubility	S
Spry drying	SD
Total Phenols	TP
Trolox equivalent	TE
Wettability	$\underline{W_e}$

References

[1] D.S. Ferreira, V. Rosso, A.Z. Mercadante, Compostos bioativos presentes em amora-preta (*Rubus* spp.), Rev. Bras. Frutic. 32 (2010) 664–674, https://doi.org/10.1590/s0100-29452010005000110.
[2] F. Giampieri, S. Tulipani, J.M. Alvarez-Suarez, J.L. Quiles, B. Mezzetti, M. Battino, The strawberry: composition, nutritional quality, and impact on human health, Nutr 28 (2012) 9–19, https://doi.org/10.1016/j.nut.2011.08.009.
[3] B. Baby, P. Antony, R. Vijayan, Antioxidant and anticancer properties of berries, Crit. Rev. Food Sci. Nutr. 58 (15) (2018) 2491–2507, https://doi.org/10.1080/10408398.2017.1329198.
[4] V. Gowd, T. Bao, L. Wang, Y. Huang, S. Chen, X. Zheng, S. Cui, W. Chen, Antioxidant and antidiabetic activity of blackberry after gastrointestinal digestion and human gut microbiota fermentation, Food Chem. 269 (2018) 618–627, https://doi.org/10.1016/j.foodchem.2018.07.020.
[5] M. Schulz, J.F. Chim, Nutritional and bioactive value of Rubus berries, Food Biosc 31 (2019), 100438, https://doi.org/10.1016/j.fbio.2019.100438.
[6] B. Bhandari, N. Bansal, M. Zhang, P. Schuck, Handbook of Food Powders: Processes and Properties (2013) https://doi.org/10.1533/9780857098672.

[7] W. Pietsch, Agglomeration Processes: Phenomena, Technologies, Equipment. Wiley-VCH (2002).
[8] D. Ríos-Morales, C. Castillo-Araiza, R. Ruiz-Martínez, M. Vizcarra-Mendoza, Statistical evaluation and modeling of the behavior of a fluidised bed granulator, Rev. Mexicana de Ingeniería Química 10 (2011) 235–245.
[9] A. Barkouti, C. Turchiuli, J.A. Carcel, E. Dumoulin, Milk powder agglomerate growth and properties in fluidised bed agglomeration Milk powder agglomerate growth and properties in fluidised bed agglomeration, Dairy Sci. Technol. 93 (2013) 523–535, https://doi.org/10.1007/s13594-013-0132-7.
[10] W. Pietsch, Agglomeration in Industry: Occurrence and Applications. Wiley-VCH. (2005) https://doi.org/10.1002/9783527619795.
[11] B. Wang, H. Li, J. Xiang, J. Zheng, J. Wang, Fabrication of agglomerated lactose using fluidised bed for good compressibility, J. Nanomater. 4 (2021) 1–6, https://doi.org/10.1155/2021/9918847.
[12] K. Andreola, C.A. Da Silva, O.P. Taranto, Agglomeration process of rice protein concentrate using glucomannan as binder: in-line monitoring of particle size, Chem. Eng. Res. Des. 135 (2018) 37–51, https://doi.org/10.1016/j.cherd.2018.05.019.
[13] K. Haas, T. Dohnal, P. Andreu, E. Zehetner, A. Kiesslich, M. Volkert, P. Fryer, H. Jaeger, Particle engineering for improved stability and handling properties of carrot concentrate powders using fluidised bed granulation and agglomeration, Powder Technol. 370 (2020) 104–115, https://doi.org/10.1016/j.powtec.2020.04.065.
[14] T.A.M. Hirata, G.C. Dacanal, F.C. Menegalli, Effect of operational conditions on the properties of pectin powder agglomerated in pulsed fluid bed, Powder Technol. 245 (2013) 174–181, https://doi.org/10.1016/j.powtec.2013.04.047.
[15] C. De los Ríos-Carvajal, M. Cortés-Rodríguez, J.C. Arango-Tobón, Physicochemical quality and antioxidant activity of blackberry suspensions: compositional and process effects, J. Food Process. Preserv. 45 (6) (2021), e15498, https://doi.org/10.1111/jfpp.15498.
[16] M. Cortés-Rodríguez, J.H. Gil G, R. Ortega-Toro, Influence of the feed composition and the spray drying process on the quality of a powdered mixture of blackberry (*Rubus glaucous* Benth), Rev. Mex. Ing. Quim. 21 (3) (2022) 1–17, https://doi.org/10.24275/rmiq/Alim2855.
[17] MinSalud, Ministerio de Salud y Protección Social. Resolución No. 810 de 2021. (2021) 50.
[18] Association of Official Analytical Chemists A. Official Methods of Analysis: Official Method for Moisture. Method No. 925.10 (1995). Association of Official Analytical Chemists, Washington DC.
[19] M. Cano-Chauca, P.C. Stringheta, A.M. Ramos, J. Cal-Vidal, Effect of the carriers on the microstructure of mango powder obtained by spray drying and its functional characterization, Innov. Food Sci. Emerg. Technol. 6 (2005) 420–428, https://doi.org/10.1016/j.ifset.2005.05.003.
[20] K. Sarabandi, S.M. Jafari, A.S. Mahoonak, A. Mohammadi, Application of gum Arabic and maltodextrin for encapsulation of eggplant peel extract as a natural antioxidant and color source, Int. J. Biol. Macromol. 140 (2019) 59–68, https://doi.org/10.1016/j.ijbiomac.2019.08.133.
[21] D. Pereira, C. Beres, F. Gomes, R.V. Tonon, L. Cabral, Spray drying of juçara pulp aiming to obtain a "pure" powdered pulp without using carrier agents, Dry. Technol. 38 (2020) 1175–1185, https://doi.org/10.1080/07373937.2019.1625363.
[22] D. Da Silva, C. Itoda, C. Franco, A. Pelaes, L. Yamamoto, L. Yamamoto, R. Vasconcelos, P. Matumoto-Pintro, Effects of blackberries (*Rupus* sp.; cv. Xavante) processing on its physicochemical properties, phenolic contents and antioxidant activity, J. Food Sci. Technol. 55 (11) (2018) 4642–4649, https://doi.org/10.1007/s13197-018-3405-6.
[23] Z. Fang, Y. Zhang, Y. Lü, G. Ma, J. Chen, D. Liu, X. Ye, Phenolic compounds and antioxidant capacities of bayberry juices, Food Chem. 113 (2009) 884–888, https://doi.org/10.1016/j.foodchem.2008.07.102.
[24] G. Rodríguez-Gutiérrez, J.C. Cardoso, F. Rubio-Senent, A. Serrano, R. Borja, J. Fernández-Bolaños, F.G. Fermoso, Thermally-treated strawberry extrudate: a rich source of antioxidant phenols and sugars, Innov. Food Sci. Emerg. Technol. 51 (2019) 186–193, https://doi.org/10.1016/j.ifset.2018.05.017.
[25] L.M. Rayo, L. Chaguri e Carvalho, F. Sardá, G.C. Dacanal, E.W. Menezes, C. Tadini, Production of instant green banana flour (Musa cavendischii, var. Nanicão) by a pulsed-fluidised bed agglomeration, J. Food Sci. Technol. 63 (2015) 461–469, https://doi.org/10.1016/j.lwt.2015.03.059.
[26] A.A. Santana, L.G.P. Martin, R.A. de Oliveira, L.E. Kurozawa, K.J. Park, Spray drying of babassu coconut milk using different carrier agents, Dry. Technol. 35 (2017) 76–87, https://doi.org/10.1080/07373937.2016.1160111.
[27] E. Ermiş, Food Powders: Properties and Characterization. Springer (2015) https://doi.org/10.15237/gida.gd14072.
[28] J. Du, A. Bück, E. Tsotsas, Influence of process variables on spray agglomeration process in a continuously operated horizontal fluidised bed, Powder Technol. 363 (2020) 195–206, https://doi.org/10.1016/j.powtec.2020.01.008.
[29] J.G. Rosa, M.F. Ávila, R.F. Nascimento, O.P. Taranto, Analysis of particle growth kinetic of pea protein isolate in fluidised bed by In-line monitoring of particle size, Chem. Eng. Trans. 74 (2019) 409–414, https://doi.org/10.3303/CET1974069.
[30] K. Andreola, C.A.M. Da Silva, O.P. Taranto, Production of instant rice protein concentrate by rotating pulsed fluidised bed agglomeration using hydrolysed collagen solution as binder, Chem. Eng. Trans. 49 (2016) 115–120, https://doi.org/10.3303/CET1649020.
[31] C.E. De Farias, R.V. Correia, L. Caetano, R.B. de Oliveira, N.A. Pereira, F.C. da Silva, F. Pimentel, A.K. De Souza, K. Andreola, O.P. Taranto, Combining fruit pulp and rice protein agglomerated with collagen to potentialize it as a functional food: particle characterization, pulp formulation and sensory analysis, J. Food Sci. Technol. 58 (2021) 4194–4204, https://doi.org/10.1007/s13197-020-04892-7.
[32] M. Langner, I. Kitzmann, A. Ruppert, I. Wittich, B. Wolf, In-line particle size measurement and process influence on rotary fluidised bed agglomeration, Powder Technol. 364 (2020) 673–679, https://doi.org/10.1016/j.powtec.2020.02.034.
[33] M. Dadkhah, E. Tsotsas, Influence of process variables on internal particle structure in spray fluidised bed agglomeration, Powder Technol. 258 (2014) 165–173, https://doi.org/10.1016/j.powtec.2014.03.005.
[34] J. Ji, J. Fitzpatrick, K. Cronin, P. Maguire, H. Zhang, S. Miao, Rehydration behaviours of high protein dairy powders: the influence of agglomeration on wettability, dispersibility and solubility, Food Hydrocoll 58 (2016) 194–203, https://doi.org/10.1016/j.foodhyd.2016.02.030.
[35] C. Turchiuli, Z. Eloualia, N. El Mansouri, E. Dumoulin, Fluidised bed agglomeration: agglomerates shape and end-use properties, Powder Technol. 157 (2005) 168–175, https://doi.org/10.1016/j.powtec.2005.05.024.
[36] S. Kanchi, S. Ahmed, M. I. Sabela, C. Hussain, Nanomaterials: biomedical, environmental, and engineering applications. In Nanomaterials: Biomedical, Environmental and Engineering Applications (2018), https://doi.org/10.1002/9781119-370383.
[37] K. Dhanalakshmi, S. Ghosal, S. Bhattacharya, Agglomeration of food powder and Applications, Crit. Rev. Food Sci. Nutr. 51 (2011) 432–441, https://doi.org/10.1080/10408391003646270.
[38] E. Zhalehrajabi, K.K. Lau, K. Zilati, S.M. Zahraee, S.H. Seyedin, B. Azeem, A. Shaaban, Effect of biodegradable binder properties and operating conditions on growth of urea particles in a fluidised bed granulator, Mater 12 (2019) 1–25, https://doi.org/10.3390/ma12142320.
[39] J. L. Villacrez, Desarrollo de microencapsulados por spray drying a partir de frutos de mora de castilla (*Rubus glaucus* Benth). Universidad Nacional de Colombia (2013) https://repositorio.unal.edu.co/handle/unal/52827.
[40] L. Forny, A. Marabi, S. Palzer, Wetting, disintegration and dissolution of agglomerated water soluble powders, Powder Technol. 206 (2011) 72–78, https://doi.org/10.1016/j.powtec.2010.07.022.
[41] I. Atalar, F. Yazici, Effect of different binders on reconstitution behaviors and physical, structural, and morphological properties of fluidised bed agglomerated yoghurt powder, Dry. Technol. 37 (2018) 1656–1664, https://doi.org/10.1080/07373937.2018-1529038.
[42] I. Atalar, A. Kurt, F. Saricaoğlu, O. Gül, H. Genççelep, Agglomerated mushroom (*Agaricus bisporus*) powder: optimization of top spray fluidised bed agglomeration conditions, J. Food Process. Eng. 44 (2021), 13687, https://doi.org/10.1111/jfpe.13687.
[43] H. Lee, B. Yoo, Agglomerated xanthan gum powder used as a food thickener: effect of sugar binders on physical, microstructural, and rheological properties, Powder Technol. 3 (2020) 301–306, https://doi.org/10.1016/j.powtec.2019.11.124.
[44] H. Lee, B. Yoo, Agglomeration of galactomannan gum powders: physical, rheological, and structural characterizations, 256 Carbohydr, Polym (2021), 117599, https://doi.org/10.1016/j.carbpol.2020.117599.
[45] H. Yuksel, S.N. Dirim, Application of the agglomeration process on spinach juice powders obtained using spray drying method, Dry. Technol. 39 (2020) 19–34, https://doi.org/10.1080/07373937.2020.1832515.
[46] L. Benelli, W.P. Oliveira, Fluidised bed coating of inert cores with a lipid-based system loaded with a polyphenol-rich Rosmarinus officinalis extract, Food Bioprod. Process. 114 (2019) 216–226, https://doi.org/10.1016/j.fbp.2019.01.004.

[47] G.Y. Jeong, J.H. Bak, B. Yoo, Physical and rheological properties of xanthan gum agglomerated in fluidised bed: effect of HPMC as a binder, Int. J. Biol. Macromol. 121 (2019) 424–428, https://doi.org/10.1016/j.ijbiomac.2018.10.048.
[48] M. Benkovic, A.J. Tusek, A. Belscak-Cvitanovic, A. Lenart, E. Domian, D. Komes, I. Bauman, Artificial neural network modelling of changes in physical and chemical properties of cocoa powder mixtures during agglomeration, Food Sci. Technol. 64 (2015) 140–148, https://doi.org/10.1016/j.lwt.2015.05.028.
[49] D.J. McSweeney, V. Maidannyk, J.A. O'Mahony, N.A. McCarthy, Rehydration properties of regular and agglomerated milk protein concentrate powders produced using nitrogen gas injection prior to spray drying, J. Food Eng. 305 (2021), 110597, https://doi.org/10.1016/j.jfoodeng.2021.110597.
[50] H. Yan, G.V. Barbosa-Cánovas, Compression characteristics of agglomerated food powders: effect of agglomerate size and water activity, Food Sci. Technol. Int. 3 (1997) 351–359, https://doi.org/10.1177/108201329700300506.
[51] V.S. Farias-Cervantes, A. Chávez-Rodríguez, P.A. García-Salcedo, P.M. García-López, J. Casas-Solís, I. Andrade-González, Antimicrobial effect and in vitro release of anthocyanins from berries and Roselle obtained via microencapsulation by spray drying, J. Food Process. Preserv. 42 (2018) 1–8, https://doi.org/10.1111/jfpp.13713.
[52] A. Horszwald, H. Julien, W. Andlauer, Characterisation of Aronia powders obtained by different drying processes, Food Chem. 141 (2013) 2858–2863, https://doi.org/10.1016/j.foodchem.2013.05.103.
[53] S.S. Santos, L.M. Rodrigues, S.C. Costa, R.C. Bergamasco, G.S. Madrona, Microencapsulation of bioactive compounds from blackberry pomace (*Rubus fruticosus*) by spray drying technique, Int. J. Food Eng. 13 (2017) 1–11, https://doi.org/10.1515/ijfe-2017-0047.
[54] A. Sadowska, F. Świderski, E. Hallmann, Bioactive, physicochemical and sensory properties as well as microstructure of organic strawberry powders obtained by various drying methods, Appl. Sci. 10 (2020) 9–12, https://doi.org/10.3390/app10144706.
[55] P. Vonghirundecha, S. Chusri, P. Meunprasertdee, T. Kaewmanee, Microencapsulated functional ingredients from a Moringa oleifera leaf polyphenol-rich extract: characterization, antioxidant properties, in vitro simulated digestion, and storage stability, J. Food Sci. Technol. 154 (2021), 112820, https://doi.org/10.1016/j.lwt.2021.112820.
[56] M.Z. Islam, Y. Kitamura, Y. Yamano, M. Kitamura, Effect of vacuum spray drying on the physicochemical properties, water sorption and glass transition phenomenon of orange juice powder, J. Food Eng. 169 (2016) 131–140, https://doi.org/10.1016/j.jfoodeng.2015.08.024.
[57] J. Gamboa-Santos, R. Megías-Pérez, A.C. Soria, A. Olano, A. Montilla, M. Villamiel, Impact of processing conditions on the kinetic of vitamin C degradation and 2-furoylmethyl amino acid formation in dried strawberries, Food Chem. 153 (2014) 164–170, https://doi.org/10.1016/j.foodchem.2013.12.004.
[58] E. Dłuzewska, A. Florowska, E. Domian, M. Wojciechowska, M. Maszewska, The influence of the agglomeration process on stability of microencapsulated β-Carotene, Int. J. Food Eng. 16 (2020) 1–10, https://doi.org/10.1515/ijfe-2018-0310.
[59] G.F. Nogueira, C.T. Soares, L.G. Martin, F.M. Fakhouri, R.A. de Oliveira, Influence of spray drying on bioactive compounds of blackberry pulp microencapsulated with arrowroot starch and gum Arabic mixture, J. Microencapsul. 37 (2020) 65–76, https://doi.org/10.1080/02652048.2019.1693646.
[60] G. V. Barbosa-Cánovas, E. Ortega-Rivas, P. Juliano, H. Yan, Food powders: physical properties, processing, and functionality. In Food Powders. Kluwer Academic/Plenum Publishers (2005), https://doi.org/10.1007/0-387-27613-0.
[61] C. Anandharamakrishnan, S. P. Ishwarya, Spray Drying Techniques for Food Ingredient Encapsulation. Wiley-Blackwell (2015).
[62] K. Šavikin, N. Nastić, T. Janković, D. Bigović, B. Miličević, S. Vidović, N. Menković, J. Vladić, Effect of type and concentration of carrier material on the encapsulation of pomegranate peel using spray drying method, Foods 10 (2021) 1–11, https://doi.org/10.3390/foods10091968.
[63] G.C. Dacanal, T.A. Hirata, F.C. Menegalli, Fluid dynamics and morphological characterization of soy protein isolate particles obtained by agglomeration in pulsed- fluid bed, Powder Technol. 247 (2013) 222–230, https://doi.org/10.1016/j.powtec.2013.07.001.
[64] K. Thirugnanasambandham, V. Sivakumar, Influence of process conditions on the physicochemical properties of pomegranate juice in spray drying process: modelling and optimization, J. Saudi Soc. Agric. Sci. 16 (2015) 358–366, https://doi.org/10.1016/j.jssas.2015.11.005.